CHMP5 is essential for late endosome function and down-regulation of receptor signaling during mouse embryogenesis

Jae-Hyuck Shim,[1,2] Changchun Xiao,[1,2] Matthew S. Hayden,[1,2] Ki-Young Lee,[1,2] E. Sergio Trombetta,[3] Marc Pypaert,[3] Atsuki Nara,[4] Tamotsu Yoshimori,[4] Bettina Wilm,[5] Hediye Erdjument-Bromage,[6] Paul Tempst,[6] Brigid L.M. Hogan,[5] Ira Mellman,[3] and Sankar Ghosh[1,2]

[1]Section of Immunobiology, [2]Department of Molecular Biophysics and Biochemistry, and [3]Department of Cell Biology, Ludwig Institute for Cancer Research, Yale University School of Medicine, New Haven, CT 06520
[4]Division of Cell Genetics, National Institute for Genetics, Mishima, 411-8540, Japan
[5]Department of Cell Biology, Vanderbilt University Medical Center, Nashville, TN 37232
[6]Memorial Sloan-Kettering Cancer Center, New York, NY 10021

Charged MVB protein 5 (CHMP5) is a coiled coil protein homologous to the yeast Vps60/Mos10 gene and other ESCRT-III complex members, although its precise function in either yeast or mammalian cells is unknown. We deleted the CHMP5 gene in mice, resulting in a phenotype of early embryonic lethality, reflecting defective late endosome function and dysregulation of signal transduction. *Chmp5*$^{-/-}$ cells exhibit enlarged late endosomal compartments that contain abundant internal vesicles expressing proteins that are characteristic of late endosomes and lysosomes. This is in contrast to ESCRT-III mutants in yeast, which are defective in multivesicular body (MVB) formation. The degradative capacity of *Chmp5*$^{-/-}$ cells was reduced, and undigested proteins from multiple pathways accumulated in enlarged MVBs that failed to traffic their cargo to lysosomes. Therefore, CHMP5 regulates late endosome function downstream of MVB formation, and the loss of CHMP5 enhances signal transduction by inhibiting lysosomal degradation of activated receptors.

Introduction

Genetic studies in yeast have identified a subset of *vps* (*vacuolar protein–sorting*) mutants, which are called the class E mutants. These mutants display an exaggerated prevacuolar/late endosome compartment, called the class E compartment, which is caused by defects in multivesicular body (MVB) sorting (Raymond et al., 1992). There are 17 soluble and 1 membrane class E *vps* proteins in yeast, including Vps27p, the ESCRT-I, -II, and -III complexes, Vps4p, Bro1/Vps31, Vta1, Vps60p/MOS10, and Did2/Fti1 (Babst, 2005). A recent model has proposed that monoubiquitinated receptors and cargo proteins are first recognized by Vps27p and Hse1p, which results in the sequential recruitment of three distinct multiprotein complexes, i.e., ESCRT-I, -II, and -III, to endosomal membranes from the cytosol (Katzmann et al., 2001; Babst et al., 2002a,b; Bilodeau et al., 2002). Although the details are unclear, these complexes are required for the sorting of monoubiquitinated cargo for inclusion in MVBs, as well as the formation of the MVBs themselves (for reviews see Katzmann et al., 2002; Raiborg et al., 2003). The final step in the membrane invagination that forms MVBs may be specifically associated with the ESCRT-III complex and its ability to interact with the AAA-ATPase Vps4p (Babst et al., 1998). Doa4p is a deubiquitinating enzyme that recycles ubiquitin by releasing monoubiquitin moieties before the incorporation of proteins into the internal membranes of the MVB (Amerik et al., 2000).

Several in vitro studies have investigated the protein–protein interactions of the class E Vps proteins in yeast and mammalian cells using yeast two-hybrid and GST pull-down

J.-H. Shim and C. Xiao contributed equally to this paper.

Correspondence to Sankar Ghosh: sankar.ghosh@yale.edu

C. Xiao's present address is The CBR Institute for Biomedical Research, Boston, MA 02115.

B.L.M. Hogan's present address is Dept. of Cell Biology, Duke University Medical Center, Durham, NC 27710.

Abbreviations used in this paper: CHMP5, charged MVB protein 5; CI-M6PR, cation-independent M6PR; E, embryonic day; EGFR, EGF receptor; ES, embryonic stem; HEK, human embryonic kidney; LAMP1, lysosome-associated membrane protein 1; LBPA, lysobisphosphatidic acid; M6PR, mannose 6-phosphate receptor; MEF, mouse embryonic fibroblast; MHC, major histocompatibility class; MVB, multivesicular body; SARA, Smad anchor for receptor activation; shRNA, short hairpin RNA; siRNA, small interfering RNA; TβRII, TGFβ receptor II; UIM, ubiquitin-interacting motif.

The Journal of Cell Biology, Vol. 172, No. 7, March 27, 2006 1045–1056
http://www.jcb.org/cgi/doi/10.1083/jcb.200509041

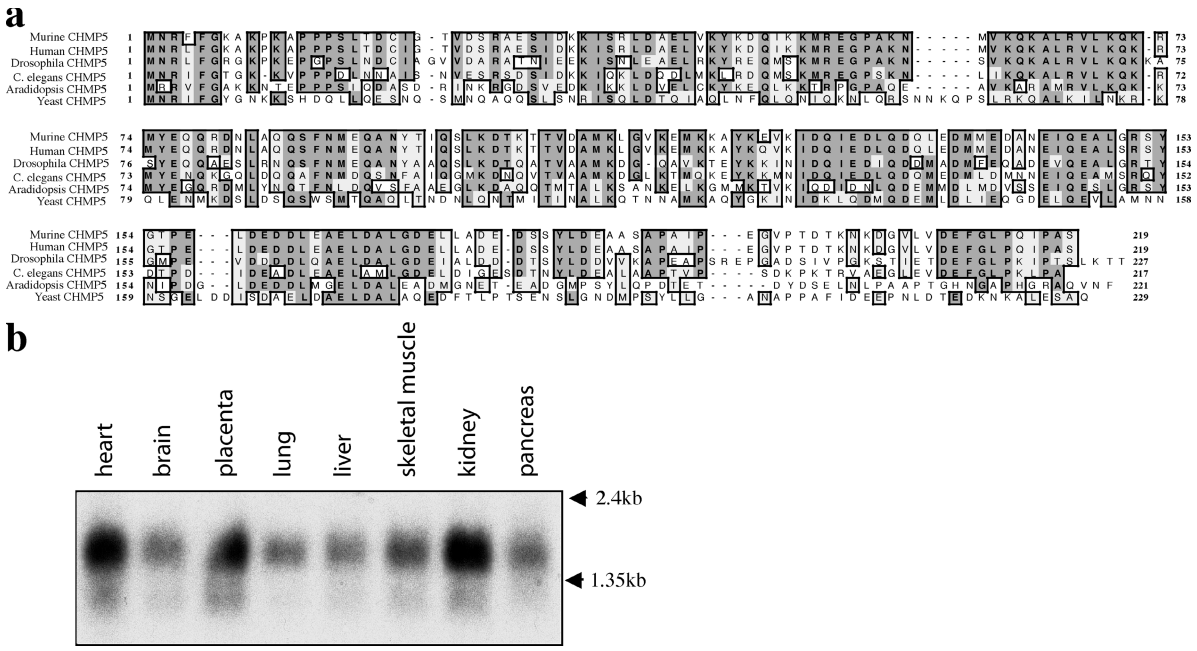

Figure 1. **Characterization of CHMP5.** (a) Protein sequence alignment of CHMP5 homologues from mouse, human, *D. melanogaster*, *C. elegans*, *A. thaliana*, and yeast. (b) Northern blot analysis of adult mouse tissues.

assays (Martin-Serrano et al., 2003; von Schwedler et al., 2003; Bowers et al., 2004). Through a coherent protein network, the ESCRT-I, -II, and -III complexes and associated proteins form a large MVB-sorting complex on endosomal membranes. The ESCRT-III complex is likely composed of two functionally distinct subcomplexes—a membrane-associated subcomplex (Vps20p–Snf7p) and a cytosolic subcomplex (Vps2p–Vps24p; Babst et al., 2002a). Recently, Did2/Fti1 and Vta1p were found to interact with Vps60p/MOS10, Vps4p, and the ESCRT-III complex, suggesting that together with Vps60p/MOS10 they play a role in regulating the activity of Vps4p and ESCRT-III (Bowers et al., 2004; Babst, 2005).

Several mammalian homologues of yeast Vps proteins have been identified (Katzmann et al., 2002). Many of these share common yeast homologues, implying a greater degree of complexity in the mammalian MVB-sorting pathway (von Schwedler et al., 2003). This may not be surprising, given the greater functional diversity and specialization that exists in animal cells. Hrs is homologous to the yeast Vps27p and recognizes ubiquitinated receptors through a conserved ubiquitin-interacting motif (UIM), which is essential for MVB sorting to degradative pathways (Polo et al., 2002). Tsg101 is homologous to yeast Vps23p, which is an ESCRT I component, and down-regulates growth factor signaling through its interaction with Hrs (Babst et al., 2000; Lu et al., 2003). The AAA-ATPase SKD1 (Vps4B) is homologous to the yeast Vps4p and regulates the association/dissociation of the MVB-sorting complex in a manner that is dependent on its ATPase activity (Babst et al., 1998; Yoshimori et al., 2000). Human Vps34 is a phosphoinositide 3 kinase that is required for internal vesicle formation within MVBs (Futter et al., 2001), and human Vps28 directly interacts with Tsg101 and is recruited to human Vps4 (E235Q)-positive endosomal membranes (Bishop and Woodman, 2001). 10 human charged MVB protein (CHMP) family proteins, which are structurally related cytosolic proteins containing coiled coil domains and are homologous to six yeast ESCRT-III components, have been identified. They have been suggested to play important roles in the final step of MVB-sorting pathways, namely the invagination of internal vesicles in MVBs, which is regulated by Vps4p (Babst, 2005). CHMP proteins also function in HIV budding, a process that is topologically similar to MVB sorting (Martin-Serrano et al., 2003; von Schwedler et al., 2003); however, the mechanism, function, and significance of CHMP proteins in mammalian MVB-sorting pathways remain to be defined.

Results

CHMP5 is expressed ubiquitously and is essential for mouse embryogenesis

We originally isolated CHMP5 as a protein that copurified with cytosolic NF-κB–IκB complexes from rabbit lung extracts. Microsequencing of this 32-kD copurifying protein revealed that it was identical to CHMP5, a CHMP family member and the mammalian homologue of yeast VPS60/MOS10 (Kranz et al., 2001). Phylogenetic analyses indicate that CHMP5 is a unique CHMP protein that is quite divergent from other CHMP family proteins (unpublished data). We began our analysis of CHMP5 by cloning and sequencing the murine and human cDNAs, which were obtained by screening a mouse liver cDNA library and by PCR from HeLa cell cDNA, respectively. CHMP5 is highly conserved through evolution and its homologues can be found in *Drosophila melanogaster*, *Caenorhabditis elegans*, *Arabidopsis thaliana*, and yeast (Fig. 1 a). CHMP5 is also ubiquitously expressed in embryonic and adult mouse tissues (not depicted and Fig. 1 b, respectively).

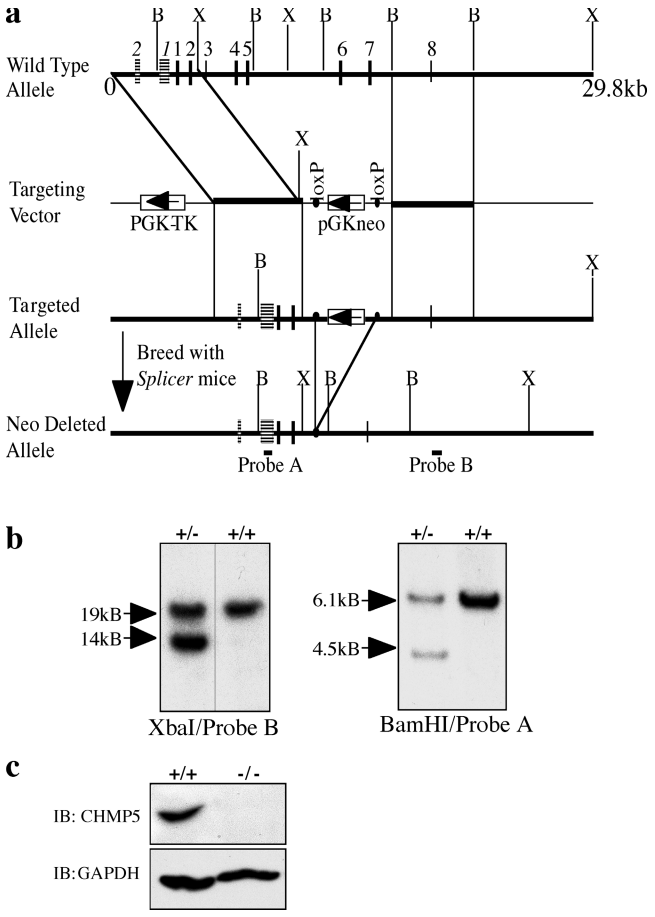

Figure 2. **Generation of *Chmp5*$^{-/-}$ embryos.** (a and b) Targeting of the *Chmp5* gene and analysis of ES clones. The targeting vector is described in Materials and methods. Note that the first two exons of the *Bag1* gene are represented by two horizontally lined boxes. Genomic DNA was digested with XbaI or BamHI and hybridized with probe B or A, respectively. The hybridized DNA fragments were 19 kb (XbaI) and 6.1 kb (BamHI) for the wild-type allele and 14 kb (XbaI) and 4.5 kb (BamHI) for the targeted allele. (c) Wild-type (+/+) and mutant (−/−) ES cell lysates were immunoblotted with antibodies specific for CHMP5 and GAPDH4.

Although the biological significance of the association of CHMP5 with the NF-κB–IκB complex remains unclear, we decided to explore the biological function of CHMP5 by generating *Chmp5*$^{-/-}$ mice. *Chmp5* genomic DNA (29.8 kb) was isolated from a 129/SvJ murine genomic DNA library using *Chmp5* cDNA as a probe. The *Chmp5* gene contains eight small exons and is separated by only 414 bp from the *Bag1* gene (Takayama and Reed, 2001). These two genes are encoded by different DNA strands, and their 5′ ends are positioned head-to-head (Fig. 2 a). To generate a null mutation of *Chmp5*, exons 3–7 of the *Chmp5* gene were replaced by a loxP-flanked neomycin-resistant gene cassette. After homologous recombination, the neo gene was deleted by crossing *Chmp5*$^{+/-}$ mice with *Splicer* mice (Fig. 2 b; Koni et al., 2001). The resulting heterozygous mice were phenotypically normal, but the homozygous mice died at approximately embryonic day 10 (E10). Most wild-type embryos and mutant littermates did not exhibit any gross morphological difference until E7.5, after which the mutant embryos displayed severe developmental abnormalities in the ventral region (Fig. 3 a). At E8.75, mutant embryos were severely disorganized, with abnormal neural tube formation, allantois-chorion fusion, and somite segmentation, although embryonic axes and structures are normal in mutant embryos (Fig. 3 b). To further analyze the anatomy of *Chmp5*$^{-/-}$ embryonic structure, we performed histological analysis of E8.5 wild-type embryos and mutant littermates (Fig. 3 c). Consistent with Fig. 3 b, severe developmental abnormalities of allantois, head fold, heart, and somite, and an apparent defect of ventral folding morphogenesis, were detected in the mutant embryos. To characterize the mutant phenotype, we performed whole-mount in situ hybridization with *Nkx2.5* as a marker of heart formation (Fig. 3 d, top) and TUNEL assay to assess cell death in E8.5 mutant embryos (Fig. 3 d, bottom). Remarkably, mutant embryos exhibited the formation of two independent hearts (cardia bifida), accompanied by massive cell death in the ventral region. These phenotypes are similar to those of murine and *D. melanogaster* embryos lacking Hrs (Table I; Komada and Soriano, 1999; Lloyd et al., 2002). These findings suggest that CHMP5, like Hrs, may play a role in regulating the endocytosis or lysosomal transport of receptors involved in signal transduction and, therefore, is indispensable for early embryonic development. However, a role for a putative ESCRT-III complex in receptor trafficking in mammalian cells is yet to be demonstrated.

CHMP5 is required for lysosomal biogenesis from late endosomes

To evaluate the involvement of CHMP5 in endocytosis, we isolated and cultured primary embryonic cells derived from E8.5 *Chmp5*$^{-/-}$ embryos. Phase-contrast microscopy indicated that *Chmp5*$^{-/-}$ cells contained enlarged vacuole-like structures (Fig. 4 a), a phenotype similar to *Hrs*$^{-/-}$ primary embryonic cells (Komada and Soriano, 1999). To characterize these structures, we performed immunofluorescence analysis with markers specific for different subcellular compartments. Immunostaining with transferrin receptor (early and recycling endosomes), EEA1 (early endosomes), TGN38 (trans-Golgi network), and Rab8 (recycling endosomes and trans-Golgi network) did not reveal any gross differences between wild-type and mutant cells (Fig. 4 a and not depicted). Further coimmunostaining with markers specific for late endosomes-MVBs and/or lysosomes, cation-independent mannose 6-phosphate receptor (M6PR; CI-M6PR), lysobisphosphatidic acid (LBPA), and lysosome-associated membrane protein 1 (LAMP1), demonstrated that

Table I. **Comparison of the phenotypes between *Chmp5* and *Hrs* mutant embryos**

Chmp5$^{-/-}$	*Hrs*$^{-/-}$
Early embryonic lethality around E10	
Most mutant embryos are smaller than the wild types at E7.5	
Defect in ventral fording morphogenesis	
Cardia bifida and massive cell death in ventral region around E8.5	
No fusion of allantois with chorion	
No somite segmentation	
Enlarged M6PR and LAMP1-positive endosomal compartments	Enlarged TfR-positive endosomal compartments
Enlarged MVBs result from heavily packed internal vesicles	Enlarged MVBs result from defect of vesicular invagination

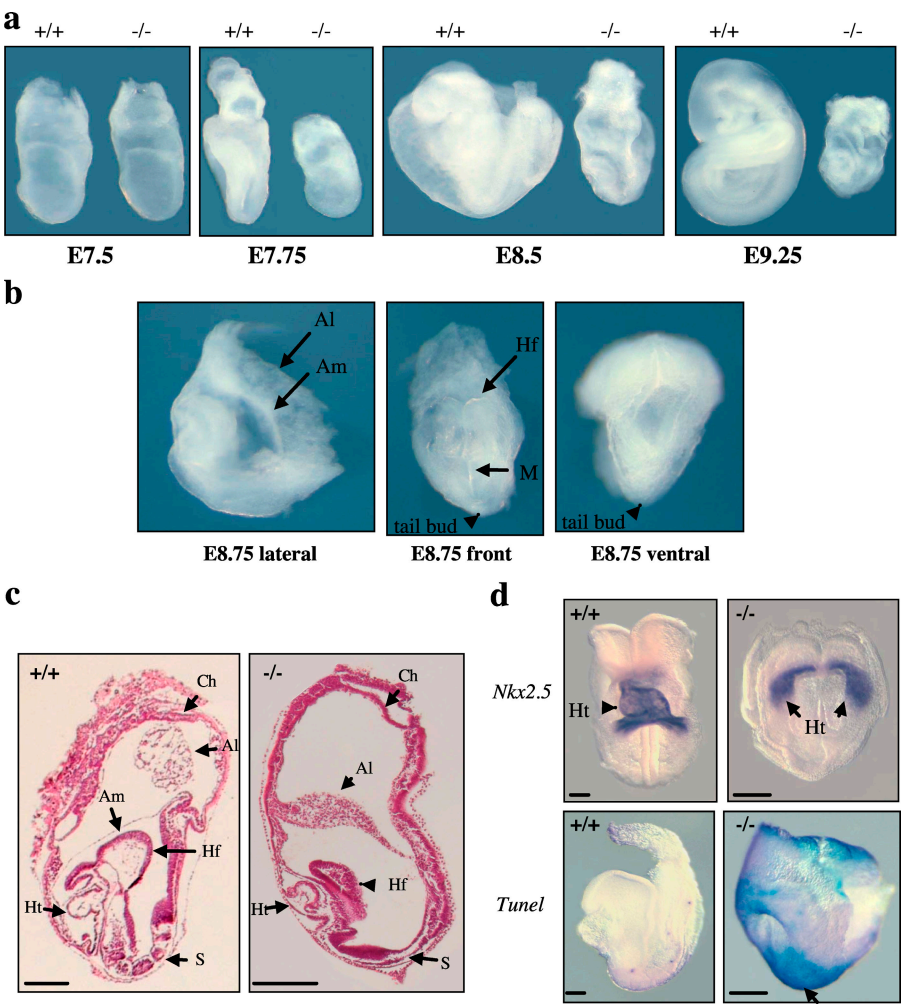

Figure 3. **Abnormal development of *Chmp5* mutant embryos.** (a) Morphological analysis of *Chmp5* mutant embryos. Lateral view of wild-type (+/+) embryos and mutant (−/−) littermates at E7.5, E7.75, E8.5, and E9.25. (b) Lateral, front, and ventral view of E8.75 *Chmp5* mutant embryos. The yolk sac was removed from the embryos. Al, allantois; Am, amnion; Hf, head fold; M, midline. (c) Histological analysis of E8.5 *Chmp5* mutant embryos. Ht, heart; S, somite. (d) Abnormal heart formation in *Chmp5* mutant embryos revealed by whole-mount in situ hybridization with the cardiac marker *Nkx2.5*. (top) Arrows and arrowhead indicate heart tissue. Massive cell death in *Chmp5* mutant embryos revealed by TUNEL staining of E8.5 embryos. (bottom) Arrow indicates apoptotic cells. Bars: (c) 50 μm; (d) 100 μm.

the vacuoles visible by phase contrast in *Chmp5*$^{-/-}$ cells were positive for CI-M6PR, LBPA, and LAMP1 (Fig. 4, b and c). Indeed, the degree of colocalization was far more pronounced in the mutant cells as compared with wild-type cells in which, as expected, distributions of CI-M6PR and LAMP1 and LBPA and LAMP1 overlapped only partially. Structures positive for CI-M6PR and lgp/LAMP1 or for LBPA and LAMP1 are generally defined as being late endosomes and as distinct from lysosomes which do not contain appreciable levels of CI-M6PR and LBPA (Kornfeld and Mellman, 1989; Kobayashi et al., 1998; Luzio et al., 2000). Thus, CHMP5 deficiency was accompanied by an accumulation of structures that appear to be late endosomes. To examine a distinct MVB-sorting pathway in *Chmp5*$^{-/-}$ cells, we performed immunostaining for major histocompatibility class (MHC) II. The majority of newly synthesized MHC II molecules are diverted from the secretory pathway upon exit from the trans-Golgi network and are directly targeted to endosomes/lysosomes (Mellman and Steinman, 2001). Mouse embryonic fibroblasts (MEFs) derived from E9.0 wild-type embryos were stimulated with IFN-γ to induce MHC II expression (Fig. 4 d; Ilangumaran et al., 2002). Wild-type and *Chmp5*$^{-/-}$ MEFs, stimulated with IFN-γ, were then stained with anti-MHC II (I-Aβ) antibody (Fig. 4 e). *Chmp5*$^{-/-}$ cells exhibit enlarged endosomes positive for MHC II molecules, whereas MHC II–positive endosomes are scattered throughout the peripheral cytoplasm in wild-type cells. Thus, CHMP5 deficiency led to the accumulation of MHC II–positive endosomes/lysosomes.

We then used transmission electron microscopy to examine MVBs in wild-type and mutant embryos. Strikingly, MVBs in the endodermal cells from the mutant embryos were abnormally enlarged and heavily packed with internal vesicles and electron-dense content, as compared with the analogous structures in cells from wild-type embryos (Fig. 4 f). Stereological analysis revealed that the fraction of total cell volume occupied by MVBs in *Chmp5*$^{-/-}$ cells was ∼1.5-fold that in wild-type cells (Fig. 4 g), confirming quantitatively that the endosomes were enlarged in the mutant cells. Interestingly, this phenotype was most clearly manifested in endodermal cells, where endocytosis is most active during embryogenesis. Collectively, these observations suggest that CHMP5 deficiency caused a global disruption in protein sorting to, or the formation of, lysosomes (M6PR^{-}/LBPA^{-}/LAMP1^{+}) from late endosomes/MVBs (M6PR^{+}/LBPA^{+}/LAMP1^{+}), rather than a specific deficit in the sorting of select proteins into lysosomes. Surprisingly, although CHMP5 deficiency affected the ability of target proteins to traffic to lysosomes, it did not prevent MVB formation.

To determine whether the block in the formation of lysosomes positive for M6PR^{-}/LBPA^{-}/LAMP1^{+} would result

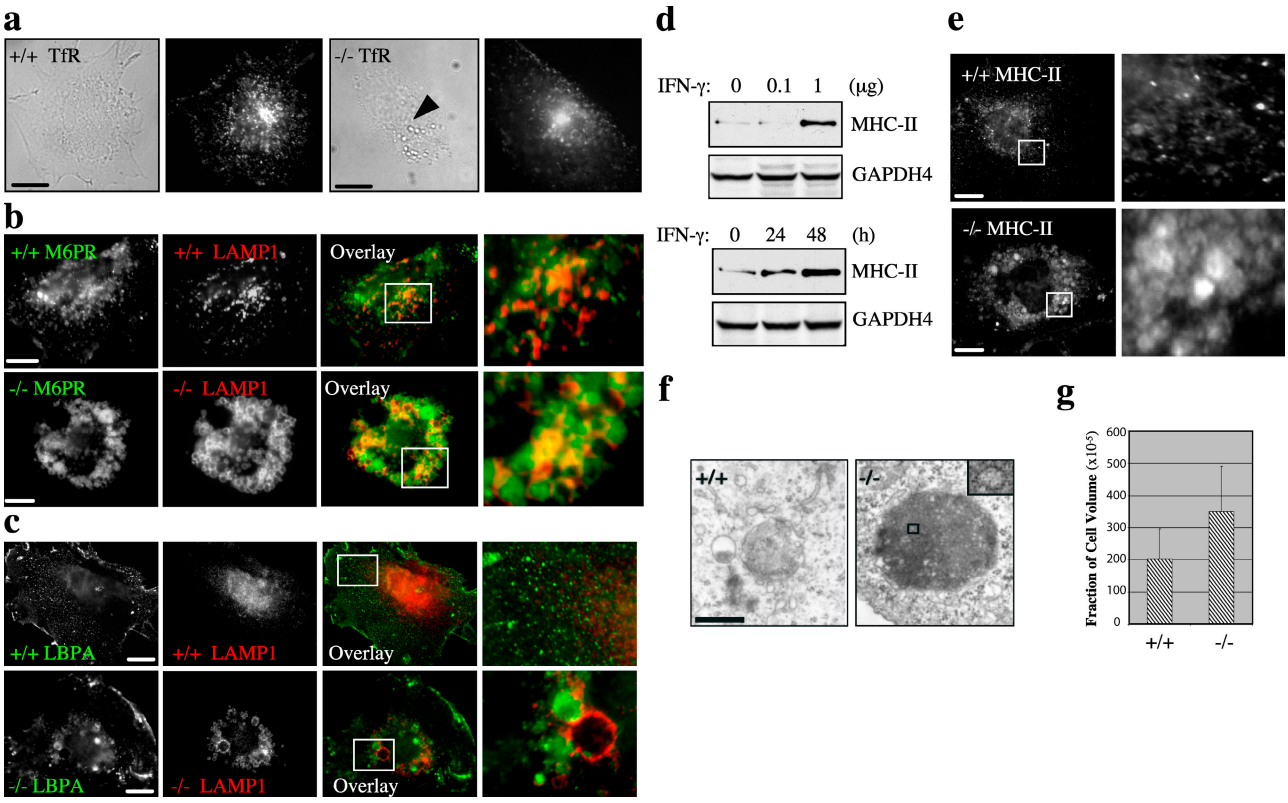

Figure 4. **CHMP5 is essential for biogenesis of lysosomes from mature MVBs.** (a–c) Immunofluorescence analysis of *Chmp5*$^{-/-}$ primary embryonic cells. Transferrin receptor (TfR), CA-MPR, LBPA, and LAMP1 are markers for early endosome, late endosome/MVB, and MVB/lysosome, respectively. Arrowheads indicate phase-lucent vacuolar structures present in the *Chmp5*$^{-/-}$ cells. (d) Induction of MHC II expression by IFN-γ. Primary cells derived from E9.0 embryos were incubated with the indicated amount of IFN-γ for 48 h (top) or incubated with 1 μg IFN-γ for the indicated time points (bottom). Expression of MHC II molecules was analyzed by immunoblotting with anti-MHC II (I-Aβ) antibody. (e) Wild-type or *Chmp5*$^{-/-}$ primary embryonic cells were stained with anti-MHC II (I-Aβ) antibody. (f) Transmission electron microscopy analysis of MVBs in the endodermal cells of E8.25 embryos. The inset shows an internal vesicle. (g) The fraction of MVBs per total cell volume was measured in endodermal layer of wild-type embryos (+/+) and mutant (−/−) littermates. Approximately 120 MVBs from the sections of six wild-type or *Chmp5*$^{-/-}$ embryos were counted. Error bars represent the SD. Bars: (a–c and e) 10 μm; (f) 500 nm.

in impaired degradative capacity in *Chmp5*$^{-/-}$ cells, we derived *Chmp5*$^{-/-}$ embryonic stem (ES) cells from the inner cell mass of blastocysts obtained by breeding *Chmp5* heterozygotes. ES cells are equivalent to E3.5 embryonic cells and the *Chmp5* mutant phenotype was therefore less dramatic in ES cells than in E8.5 embryonic cells. Both wild-type and mutant ES cells were able to internalize FITC-conjugated dextran at similar rates (unpublished data), indicating that CHMP5 was not required for fluid phase endocytosis by itself. However, *Chmp5*$^{-/-}$ ES cells exhibited a greatly reduced capacity to degrade material after internalization. After a 1-h pulse of the fluid phase marker HRP, wild-type ES cells degraded nearly all of the internalized protein after 9 h of chase. In contrast, very little of the HRP was degraded after uptake by *Chmp5*$^{-/-}$ ES cells, as determined by immunoblotting (Fig. 5 a) and flow cytometry (Fig. 5 b). Moreover, immunogold labeling of internalized HRP revealed that approximately fivefold more internalized HRP accumulated within enlarged MVBs in *Chmp5*$^{-/-}$ ES cells than in wild-type cells (Fig. 5 c). Thus, although HRP reached canonical late endosomes/MVBs, it was degraded less effectively in the absence of CHMP5.

Defective degradation of lysosomal contents could reflect either a disruption in the transport of internalized proteins to lysosomes or a lower overall proteolytic capacity. Immunoblotting of ES cell lysates with antibodies specific for cathepsin D and L revealed that they were present in equivalent amounts in wild-type and *Chmp5*$^{-/-}$ ES cells (Fig. 5 d). Thus, it appeared more likely that the defective degradative phenotype reflected inefficient delivery of endocytosed proteins to compartments containing active lysosomal hydrolases. Such a defect might also affect the normal down-regulation of signaling receptors, suggesting that the embryonic lethality of *Chmp5* deletion might reflect hyperactive signal transduction. Therefore, we examined the dynamics of TGFβ receptor II (TβRII), which has a well characterized role in early embryogenesis (Seto et al., 2002).

CHMP5 affects turnover and down-regulation of TGFβ receptors

The early embryonic lethality of *Chmp5* mutant embryos prevented us from obtaining appropriate mutant cells that could be used to study receptor turnover and signaling in vitro. We therefore used small interfering RNA (siRNA) technology to generate CHMP5 knockdown cells. Two target sequences of the *Chmp5* gene (Sh1 and Sh2; murine CHMP5) were cloned into a pSUPER.retro vector along with an H1-RNA promoter,

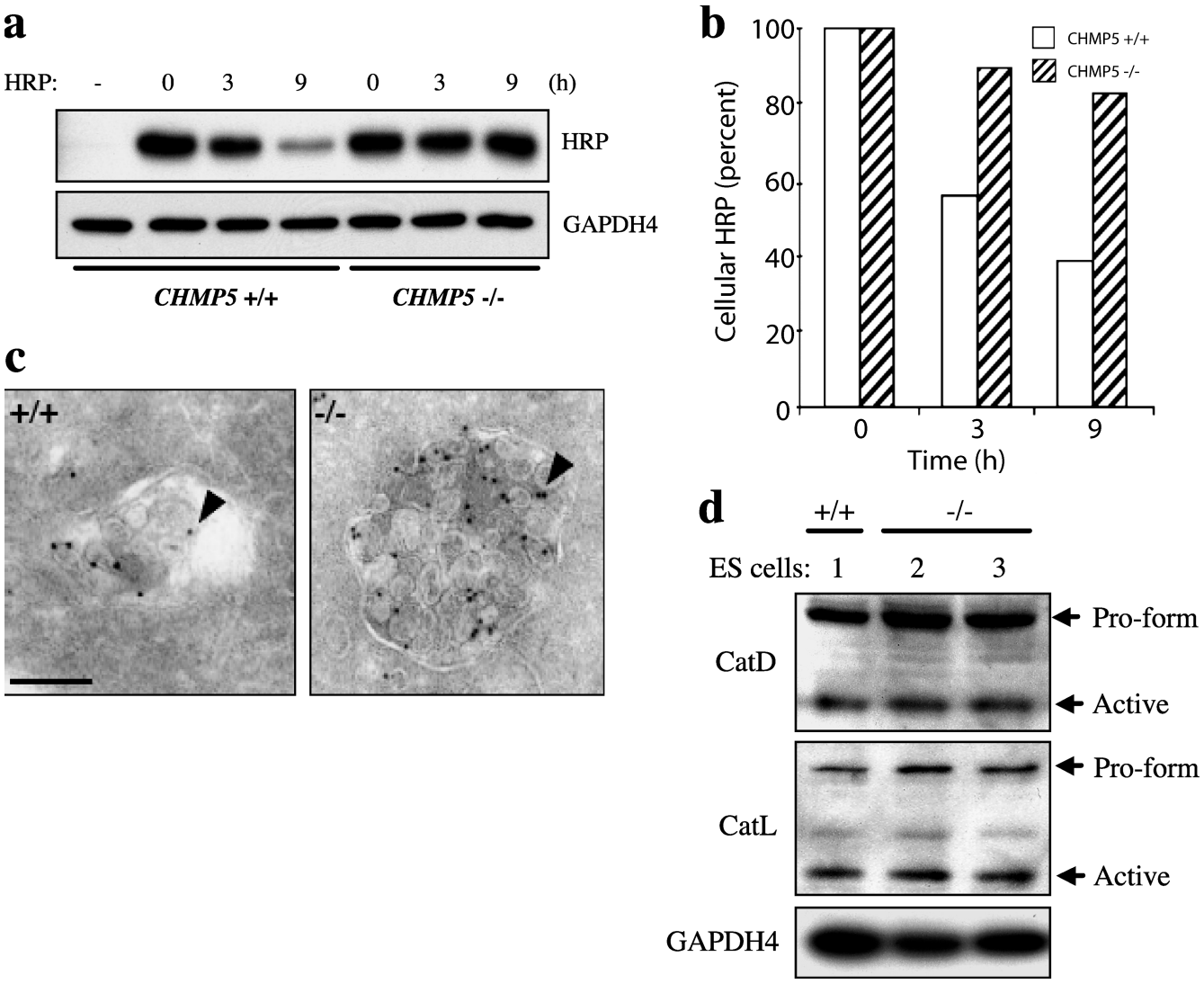

Figure 5. **CHMP5 plays a role in endosomal transport to lysosomes.** (a and b) HRP degradation is blocked in *Chmp5*$^{-/-}$ cells. ES cells cultured on 0.2% gelatin-coated plates were incubated in medium containing 100 μg/ml HRP for 1 h and then placed in normal medium (time 0). (a) Cells were lysed at the indicated time points and immunoblotted with anti-HRP antibody. (b) Alternatively, the amount of HRP remaining inside the cells was quantitatively measured by flow cytometry, and the percentage of cellular HRP was calculated based on mean fluorescence intensity. (c) Transmission electron microscopy analysis of internalized HRP in MVBs of *Chmp5*$^{-/-}$ cells. After incubation with HRP for 2 h, ES cells were fixed, sectioned, and stained with gold-conjugated anti-HRP antibody. Arrowheads indicate HRP-gold particles. (d) Lysosomal hydrolase activity in *Chmp5*$^{-/-}$ cells. Wild-type (+/+; 1) and mutant (−/−; 2 and 3) ES cells were lysed and immunoblotted with antibodies specific to cathepsin D and L. Bar, 100 nm.

which directs synthesis of short hairpin RNA (shRNA) that can be converted into an siRNA capable of knocking down target gene expression (Paddison et al., 2002). Transient transfection of the shRNAs showed that Sh2 was capable of dramatically reducing the level of transiently expressed mouse CHMP5, whereas Sh1 was inactive in this assay.

To determine if CHMP5 deficiency affects the postendocytic fate of TβRII, we transfected NIH3T3 cells with HA-tagged TβRII (HA-TβRII) in the absence or presence of Sh2 (Fig. 6 a). Receptor endocytosis was triggered by the addition of TGFβ, and receptor fate was monitored using an anti-HA monoclonal antibody that was added simultaneously to the medium, as previously described (Hayes et al., 2002; Di Guglielmo et al., 2003). Receptor distribution was analyzed relative to LAMP1 staining. In control cells, HA-TβRII was found largely in LAMP1-negative endosomes scattered throughout the peripheral cytoplasm, reflecting internalization of the receptor and its degradation in lysosomes. In CHMP5 knockdown cells, however, TβRII was more abundant and was often associated with enlarged, LAMP1-positive structures typical of the enlarged late endosomes/MVBs seen in *Chmp5*$^{-/-}$ cells. At least at the level of immunofluorescence, the receptor appeared to reside within the endosomal lumen as well as on the limiting membrane. Consistent with this, a recent report has also shown that GFP-tagged CHMP5 protein, which is a putative CHMP5 dominant-negative mutant, leads to accumulation of ligand-bound EGF receptor (EGFR) in enlarged perinuclear vesicles and a delay in EGFR degradation (Ward et al., 2005).

To determine localization of TβRII in these endosomes, we performed a protease protection assay on subcellular fractions

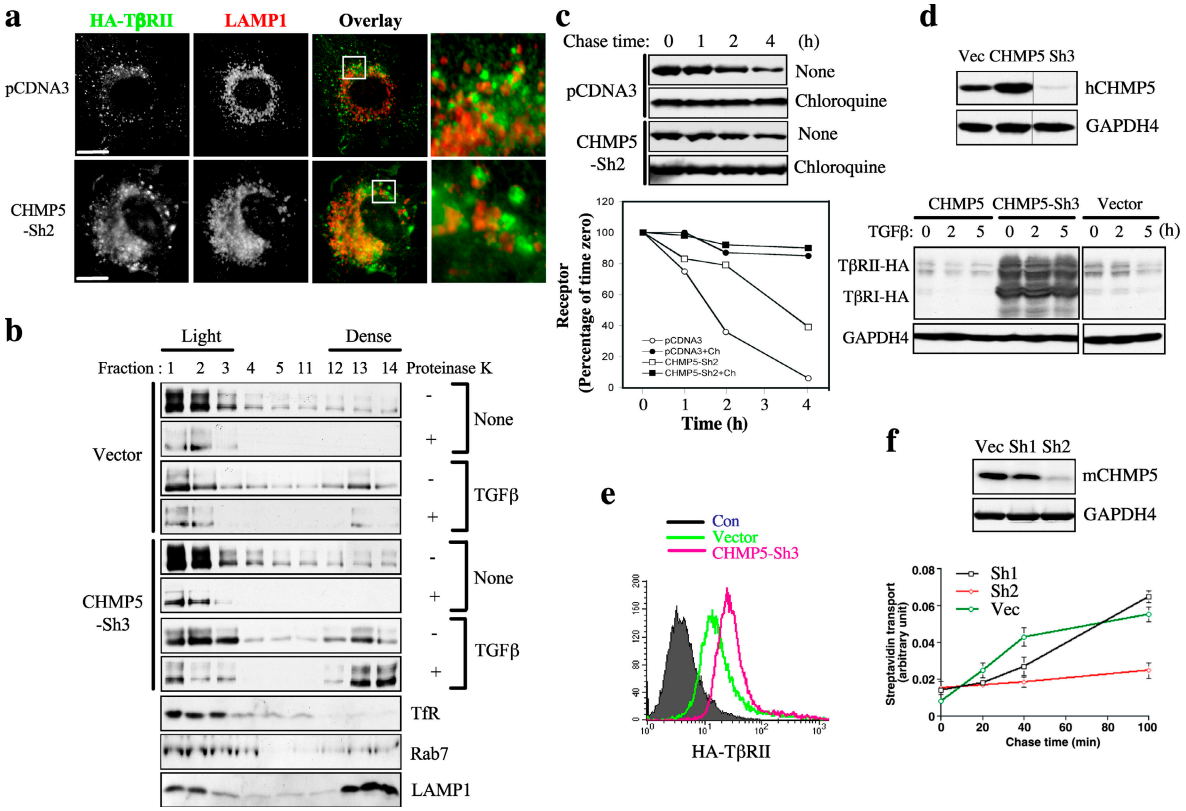

Figure 6. **CHMP5 plays a role in down-regulation of TGFβ receptors.** (a) Subcellular distribution of TβRII in CHMP5 knockdown cells. NIH3T3 cells were transfected with extracellularly HA-TβRII in the absence or presence of murine CHMP5 shRNA (Sh2). 48 h later, cells were incubated with HA antibody, stimulated with 5 ng/ml TGFβ for 1 h, and immunostained with anti-LAMP1 antibody. (b) HEK293 cells were transfected with COOH-terminal HA-TβRII in the absence or presence of human CHMP5 shRNA (Sh3). 48 h after transfection, cells were treated with 10 ng/ml TGFβ for 5 h or left untreated, and fractionated on Percoll gradients. Transferrin receptor (TfR), Rab7, or LAMP1 was used as a marker for the plasma membrane, early or recycling endosomes, late endosomes/MVBs, or lysosomes, respectively. Each fraction was treated with proteinase K or left untreated, and HA-TβRII was analyzed by immunoblotting with anti-HA antibody. (c) NIH3T3 cells were transfected with TβRII-HA, together with control vector or murine CHMP5 shRNA (Sh2). 48 h later, cells were labeled with S^{35} methionine in the absence or presence of 0.4 mM chloroquine, and then chased for the indicated times in medium containing unlabeled methionine and 5 ng/ml TGFβ. S^{35}-labeled TβRII was immunoprecipitated with anti-HA antibody, and then analyzed by phosphorimaging. Alternatively, the HA-TβRII expression was quantified and graphed as receptor quantity (percentage of time 0) versus time. (d) HEK293 cells were transfected with control vector (Vector), CHMP5 expression vector (CHMP5), or human CHMP5 shRNAs (Sh3) and immunoblotted with antibodies specific to CHMP5 and GAPDH4 (top). HEK293 cells were transfected with TβRI-HA and TβRII-HA, together with control vector, CHMP5, or CHMP5-Sh3. 48 h after transfection, cells were treated with 10 ng/ml TGFβ for 5 h, or left untreated in the presence of 20 μM cyclohexamide before lysis, and then immunoblotted with antibodies specific to HA and GAPDH4. (e) HEK293 cells were transfected with extracellularly HA-TβRII, together with control vector or human CHMP5 shRNA (Sh3). 48 h after transfection, HA-TβRII expression was analyzed with anti-HA antibody by using flow cytometry. (f) NIH3T3 cells were incubated with biotin-conjugated HRP in medium containing protease inhibitors for 3 h to label preexisting lysosomes. 48 h after transfection with murine CHMP5 shRNAs (Sh1 and Sh2), cells were incubated with streptavidin for 10 min, washed, and chased for the indicated time. Cells were lysed with biotin-containing lysis buffer and HRP enzymatic activity was measured using ELISA on anti–streptavidin-coated plates. Endogenous murine CHMP5 protein level was analyzed by immunoblotting with anti-CHMP5 antibody (top). Error bars represent the SD. $n = 3$.

of cells expressing COOH-terminal HA-TβRII along with control vector or human CHMP5 shRNA (Sh3; Fig. 6 b). Percoll gradients allowed a separation of a light fraction containing the plasma membrane, early/recycling endosomes, and a population of $Rab7^+$ or $LAMP1^+$ endosomes from denser fractions containing $Rab7^+$ late endosomes, as well as $LAMP1^+$ lysosomes (Mellman, 1996). In control cells, the majority of the HA-TβRII was, as expected, detected in the light fraction (i.e., at the plasma membrane) in the absence of TGFβ stimulation. After TGFβ addition for 5 h, the total amount of receptor was greatly decreased because of degradation, but some of the remaining HA-TβRII was detected in the dense fractions, consistent with ligand-induced internalization and delivery to lysosomes. The majority of HA-TβRII, particularly in the light-density plasma membrane–containing fractions, was sensitive to proteinase K treatment.

A different picture emerged in cells lacking CHMP5. First, consistent with our analysis of steady-state (Fig. 6 d) and cell surface expression (Fig. 6 e) of TβRII receptors, HA-TβRII levels were significantly increased in CHMP5 knockdown cells. Importantly, after TGFβ treatment the HA-TβRII that appeared in the denser fractions was now protected from degradation by proteinase K. Thus, at least a portion of the HA-TβRII that accumulates after ligand-induced receptor internalization appears to be localized within the lumen of Percoll-dense compartments, likely MVBs. Together with our morphological experiments, these data suggest that CHMP5 deficiency leads to the accumulation of internalized TβRII, at least, in part, on the internal membranes of late endosomal MVBs.

The increased staining of the HA-TβRII suggested that CHMP5 knockdown interfered with the normal down-regulation

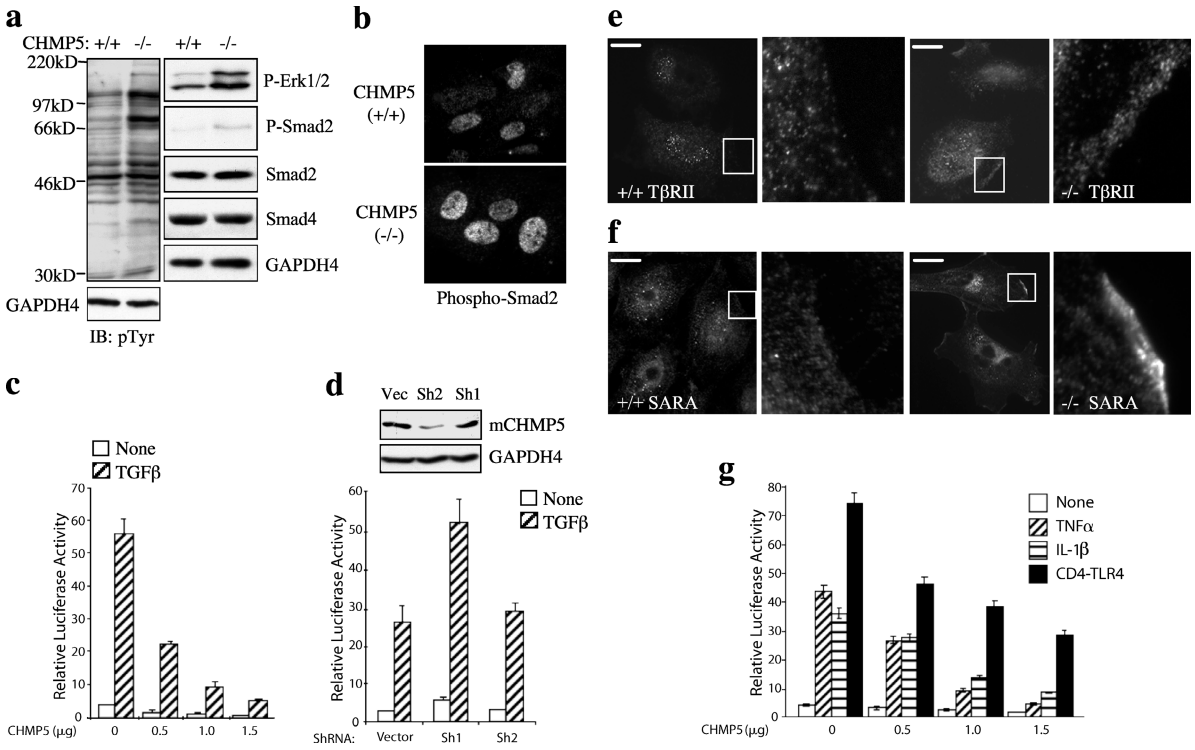

Figure 7. **CHMP5 regulates multiple signaling pathways.** (a) Hyperactivation of multiple signaling pathways in *Chmp5*$^{-/-}$ embryos. Extracts from E8.5 wild-type (+/+) and mutant (−/−) embryos were immunoblotted with antibodies specific to phosphotyrosine (pY), phospho-Erk1/2 (P-Erk1/2), phospho-Smad2 (P-Smad2), Smad2, Smad4, and GAPDH4. (b) Nuclear localization of phosphorylated Smad2 in *Chmp5*$^{-/-}$ primary embryonic cells. Wild-type (+/+) and *Chmp5*$^{-/-}$ (−/−) cells were stained with anti–phospho-Smad2 antibody. Images were obtained by a fluorescence microscope using a 40× objective. (c) NMuMg cells were transfected with the 3TP-lux reporter together with the indicated amounts of CHMP5 expression vector. Cells were treated with 1 ng/ml TGFβ for 24 h before lysis and then analyzed for luciferase activity. (d) NMuMG cells were transfected with murine CHMP5 shRNAs (Sh2 and Sh1) or control vector (Vector) and assayed as in c. Endogenous CHMP5 protein level was analyzed by immunoblotting with anti-CHMP5 antibody. (e and f) Distributions of TβRII and SARA in *Chmp5*$^{-/-}$ primary embryonic cells. Wild-type (+/+) and *Chmp5*$^{-/-}$ (−/−) cells were stained with antibodies specific for TβRII (e) and SARA (f). (g) HEK293 cells were transfected with pBIIX-luc reporter together with the indicated amounts of CHMP5 expression vector. Cells were treated with 10 ng/ml TNFα or10 ng/ml IL-1β for 4 h before lysis and then analyzed for luciferase activity. Alternatively, cells were transfected with pBIIX-luc reporter, CD4-TLR4 expression vector, and the indicated amounts of CHMP5 expression vector. Luciferase activity was assayed 24 h after transfection. (c, d, and g) Error bars represent the SD. $n = 3$. Bars, 20 μm.

of the receptor after ligand binding. To test this hypothesis, we transfected NIH3T3 cells with HA-TβRII, together with either control vector or Sh2, and assessed receptor turnover using pulse-chase analysis (Fig. 6 c). Consistent with a previous study showing that chloroquine significantly increases the stabilization of endogenous TGFβ receptors (Kavsak et al., 2000), treatment of cells with chloroquine blocked degradation of HA-TβRII receptors in cells expressing either control vector or mouse Sh2. In cells expressing the control vector, the half-life of HA-TβRII receptors was ∼1.5 h, whereas in cells where CHMP5 was knocked down, the half-life was extended to ∼3.5 h. To further characterize the effect of CHMP5 expression on TGFβ receptor turnover, we determined receptor levels in human embryonic kidney 293 (HEK293) cells that had been transfected with vectors encoding either wild-type CHMP5 or Sh3. The resulting cells slightly overexpressed or dramatically diminished the expression of CHMP5 protein, respectively (Fig. 6 d). Consistent with the decreased rate of degradation in NIH3T3 cells, knockdown of CHMP5 greatly increased the steady-state levels of both TβRI and TβRII (Fig. 6 d, bottom). In contrast, overexpression of CHMP5 slightly decreased the amount of receptor protein, relative to nontransfected controls. Similarly, using flow cytometry we found that CHMP5 knockdown significantly increased steady-state levels of HA-TβRII receptors on the cell surface, relative to the control vector (Fig. 6 e). Together, these findings suggest that the loss of CHMP5 slows the degradation of internalized TGFβ receptors by preventing ligand-induced down-regulation. Like internalized HRP, the receptors accumulated intracellularly in late endosomes/MVBs, which are structures normally associated with receptor degradation.

To investigate whether the defect in receptor degradation might reflect a failure of late endosomes/MVBs to fuse with preexisting lysosomes, we performed an endosome–lysosome fusion assay using shRNA to transiently knockdown CHMP5 expression. To label preexisting lysosomes, NIH3T3 cells pretreated with protease inhibitors were incubated with biotin-conjugated HRP (biotin-HRP) for 3 h, and then transfected with Sh2. 48 h later, the cells were incubated with streptavidin for 10 min, and the formation of streptavidin–biotin-HRP complexes was determined after various chase intervals. Vector and control shRNA (Sh1)–expressing cells showed increasing complex formation over time, whereas complex formation was dramatically inhibited in Sh2-expressing cells (Fig. 6 f).

Therefore, streptavidin cannot easily reach previously formed lysosomes in the absence of CHMP5, implying that CHMP5 is required for efficient fusion of late endosomes/MVBs with preexisting lysosomes.

CHMP5 down-regulates multiple signaling pathways during mouse embryogenesis

If, in fact, an alteration in receptor trafficking or degradation is responsible for the developmental phenotype associated with CHMP5 deletion, one would expect that knockout embryos would exhibit defects in TGFβ receptor signal transduction. There is evidence that TGFβ receptor signaling is regulated by endocytosis, with internalization being required for the receptor to reach an essential adaptor component, Smad anchor for receptor activation (SARA), in EEA1-positive endosomes, and to be subject to normal degradation and down-regulation after signal transmission (Hayes et al., 2002; Seto et al., 2002; Di Guglielmo et al., 2003). Moreover, signaling by FGF and TGFβ family members plays an essential role in embryogenesis at the stage when CHMP5 deficiency causes lethality (Rossant et al., 1997; Corson et al., 2003).

We investigated the activation state of these signaling pathways in *Chmp5*$^{-/-}$ embryos by examining the phosphorylation status of relevant signaling proteins. We made whole cell lysates from E8.5 wild-type and *Chmp5*$^{-/-}$ embryos and immunoblotted these extracts with phosphospecific antibodies against different proteins that are phosphorylated upon signaling. As shown in Fig. 7 a, tyrosine phosphorylation of many proteins, including Erk1/2 and Smad2, which function in growth factor and TGFβ family member signaling, respectively, was significantly enhanced in *Chmp5*$^{-/-}$ embryos. In addition, phosphorylated Smad2 was primarily localized in the nucleus of *Chmp5*$^{-/-}$ cells, unlike wild-type cells in which phosphorylated Smad2 is rarely observed (Fig. 7 b). These results suggest that signaling by growth factors and TGFβ family members is hyperactivated in *Chmp5*$^{-/-}$ embryos and it is likely that such dysregulation leads to embryonic lethality. Consistent with this hypothesis, TGFβ-mediated gene induction is significantly inhibited by CHMP5 overexpression and is increased upon CHMP5 knockdown (Fig. 7, c and d). We hypothesized that CHMP5 deficiency may facilitate recycling of TGFβ receptors to the plasma membrane by inhibiting lysosomal degradation of receptor, thereby leading to enhanced TGFβ signaling in *Chmp5*$^{-/-}$ cells. To test this hypothesis, we examined the distribution of TGFβ receptor and its signaling adaptor SARA in *Chmp5*$^{-/-}$ cells. Immunostaining analysis with antibodies specific for TβRII and SARA revealed that both TβRII and SARA accumulated on the plasma membrane of *Chmp5*$^{-/-}$ cells, although TβRII and SARA are relatively enriched in the TGN and cytosol of wild-type cells (Fig. 7, e and f). This is consistent with flow cytometric analyses, which indicated CHMP5 knockdown increases cell surface expression of HA-TβRII, relative to control (Fig. 6 e). Therefore, these results suggest that CHMP5 deficiency increases the steady-state levels of TGFβ receptor expression at the cell surface by decreasing degradation of internalized receptors. Increased cell surface expression of TGFβ receptor and its association with the key signaling adaptor SARA appears to be responsible for enhanced TGFβ signaling in *Chmp5*$^{-/-}$ cells.

We further demonstrated a generalized role for CHMP5 in down-regulation of receptor signaling pathways by monitoring NF-κB activity. The early lethality of *Chmp5*$^{-/-}$ embryos, and the inability to generate knockout mouse embryonic fibroblasts prevented us from assaying NF-κB activation in the knockout cells themselves. Therefore, we tested the role of CHMP5 in NF-κB activation in cell lines using a reporter assay system. As shown in Fig. 7 g, CHMP5 overexpression inhibits NF-κB activation induced by the inflammatory cytokines TNFα and IL-1β, as well as CD4-TLR4, a dominant active chimera of the toll-like receptor for the bacterial component lipopolysaccharide (Hayden and Ghosh, 2004). This result suggests that, similar to growth factor and TGFβ signaling, signaling to NF-κB is also regulated by endocytosis and, hence, that CHMP5 plays a role in the down-regulation of multiple signaling pathways.

Discussion

This study demonstrates that CHMP5 is essential for the final step of MVB sorting, namely the maturation of late endosomes/MVBs into lysosomes. In contrast to the related members of the yeast ESCRT-III complex, which are thought to be required for MVB formation, CHMP5 appears to be dispensable in this process; CHMP5-deficient cells contain abundant, and, indeed, enlarged, late endosomal MVBs. Instead, CHMP5 deficiency was associated with a significant reduction in degradative capacity, with a resulting accumulation of cargo proteins in enlarged MVBs. We also found that CHMP5 deficiency induces a generalized up-regulation of multiple signaling pathways that is attributable to the lack of degradation of internalized receptors. The resulting hyperactivation of growth factor–mediated signaling is likely responsible for the observed early embryonic lethality of *Chmp5*$^{-/-}$ mice.

A role for CHMP5 in late endocytic trafficking

The fact that CHMP5 was not required for MVB formation probably does not imply a fundamental difference between the ESCRT-III complexes in yeast and animal cells. Instead, it seems more likely that CHMP5 may not be a key component of the ESCRT-III complex in MVB formation. Indeed, previous in vitro studies have found that yeast Vps60p/MOS10, the closest yeast homologue to mammalian CHMP5, associates with the class E Vps protein, Vta1p, but not with the key ESCRT-III proteins (Bowers et al., 2004; Shiflett et al., 2004). Vps60p/MOS10 is, however, closely related to ESCRT-III proteins by amino acid sequence and by function, as Vps60p/MOS10 mutants exhibit a class E vacuolar phenotype (Kranz et al., 2001). Whether Vps60p/MOS10 is required for MVB formation in yeast is not clear, nor is its actual function in the vacuolar pathway.

Although not essential for cell viability, deletion of CHMP5 in mice was found to be required for normal embryonic development, indicating that this gene plays an important regulatory function. At the cellular level, however, CHMP5

deletion (or knockdown) did cause a marked phenotype (i.e., the accumulation of an expanded late endosomal MVB compartment) the failure to deliver internalized content to lysosomes, and the reduced degradation of internalized cargo proteins and receptors. Although MVB formation appeared intact in CHMP5 knockout cells, there was a nonspecific defect in the transport of multiple proteins, including fluid phase markers, MHC II, and cell surface receptors, to lysosomes. As a result, CHMP5 function seems necessary for complete MVB sorting, as it is responsible for the final conversion of late endosomal MVBs to lysosomes, rather than for the formation of MVBs themselves. Thus, CHMP5 may affect any of several possible events, including delivery of lysosomal enzymes to late endosomes, recycling of late endosomal components, or the fusion of late endosomes with hydrolase-rich lysosomes. Our data favor the latter possibility because we found that the rate of delivery of newly internalized streptavidin to lysosomal compartments containing previously internalized biotin-HRP was greatly slowed by CHMP5 depletion (Fig. 6 f).

Whatever its precise role, it is clear that CHMP5 is an important element in late endosomal function. Remarkably little is known about this protein, however. As indicated by phylogenetic analysis, CHMP5 (Vps60p/MOS10) is a unique CHMP family protein that does not belong to any subfamily of CHMP proteins. Conceivably, it may play roles beyond those described here for the endocytic pathway. The 5′ end of the *Chmp5* gene is separated by only 414 bp from opposing strands of the *Bag1* gene (Takayama and Reed, 2001), suggesting that both may be coregulated at the transcriptional level. BAG-1 is clearly involved in modulating apoptosis, cell proliferation, transcription, and cell motility as a multifunctional regulator. This implies the possibility that CHMP5 may participate in functions modulated by BAG1. In this regard, it is also interesting to note that Vps60p/MOS10 is required for the filament maturation of *Sacchoromyces cerevisiae* by targeting specific cargo proteins for degradation, whereas the yeast ESCRT-III proteins are required for early pseudohyphal growth (Kohler, 2003). We also found that CHMP5 is required for recruitment of CHMP1A (the mammalian homologue of the yeast Did2/Fti1) to endosomal membranes, where CHMP5 may complete an ESCRT-III complex formation (unpublished data). Failure of these final recruitment events may prevent the newly formed MVBs from releasing the assembled ESCRT complexes, impeding subsequent maturation of the MVBs themselves.

A role for CHMP5 in the regulation of signaling pathways during mouse embryogenesis

It is well established that degradation of cell surface receptors through endocytosis is a common mechanism of down-regulating growth factor and TGFβ receptor signaling (Katzmann et al., 2002; Seto et al., 2002). Genetic studies in *D. melanogaster* have reported that deletion of Hrs caused a defect in degradation of activated receptor tyrosine kinases, leading to enhanced tyrosine kinase signaling (Lloyd et al., 2002). However, despite the importance of the MVB-sorting pathway in receptor down-regulation, relatively little is known about the functional roles of mammalian endocytic components other than Hrs and Tsg101. Early embryonic lethality in mutant embryos has hindered genetic studies of mammalian endocytic components (Komada and Soriano, 1999; Ruland et al., 2001). Our results indicate that CHMP5 is required for down-regulation of TGFβ signaling pathways through lysosomal degradation of internalized receptors, which is consistent with in vivo results that show signaling by growth factors and TGFβ family members is hyperactivated in *Chmp5*$^{-/-}$ embryos. Indeed, *Chmp5*$^{-/-}$ cells exhibit increased steady-state levels of TGFβ receptor expression and accumulation of an essential TGFβ signaling adaptor, SARA, perhaps suggesting that CHMP5 deletion facilitates recycling of TGFβ receptors to the plasma membrane by blocking receptor degradation in lysosomes. CHMP5 deficiency also leads to accumulation of internalized/undigested TGFβ receptors within the lumen, as well as on the limiting membrane of LAMP1-positive endosomes/MVBs, after TGFβ stimulation. Consistent with our data, a recent study has also shown that a putative CHMP5-negative mutant, or a CHMP5 depletion using siRNA, perturbed the distribution of EGFR-containing late endosomes and EGFR trafficking, resulting in the accumulation of EGFR in enlarged perinuclear vesicles. In addition, loss of CHMP5 stabilized ligand-bound EGFR and increased its half-life by twofold (Ward et al., 2005). Thus, CHMP5 plays an essential role in trafficking and degradation of growth factor receptors, including TβRII and EGFR. Given that CHMP5 functions downstream of Hrs and TSG101 in endocytosis, and that much of the HA-TβRII in late endosomes/MVBs was protected from extravesicular proteinase K digestion, it seems likely that in CHMP5-deficient cells MVB sorting of internalized TGFβ receptors by Hrs/TSG101 and invagination of internal vesicles is normal. This would suggest that the MVBs to which the internalized receptors are delivered were rendered catabolically defective, secondary to a block in the fusion of lysosomes with MVBs or in the maturation of MVBs into lysosomes. Thus, in mammalian cells, the ESCRT-III complex member CHMP5 may not be required for MVB formation or cargo selection. Instead, it appears to control a late step in lysosomal biogenesis required for the transfer of internalized material to a hydrolytically active compartment, one that plays a critical role in down-regulation of signaling pathways through receptor degradation.

Materials and methods

Cells and reagents

NIH3T3 (murine fibroblast cells) and NMuMG (mammary gland cells; CRL-1636) cell lines were purchased from the American Type Culture Collection. The antibodies used were anti–phospho-Erk1/2 (Cell Signaling Technology), anti–phospho-Smad2 (Cell Signaling Technology), anti-Smad4 (Santa Cruz Biotechnology, Inc; H552), anti-Smad2 (Cell Signaling Technology), anti-M6PR (Affinity BioReagents, Inc.), anti-EEA1 (BD Biosciences), anti-TGN38 (BD Biosciences), anti–mouse transferrin receptor (BD Biosciences; C2), anti–mouse LAMP1 (BD Biosciences; ID4B), and anti-GAPDH4 (Fitzgerald Industries International). An anti-CHMP5 polyclonal antibody was generated by immunizing rabbits with a 17-aa synthetic peptide corresponding to the COOH-terminal sequence of mouse CHMP5 and affinity purified with immobilized antigen. Antibodies specific to LBPA, Rab8, and MHC II (I-Aβ) were gifts from T. Kobayashi (Institute of Physical and Chemical Research, Wako, Saitama, Japan) and I. Mellman (Yale University School of Medicine, New Haven, CT). Plasmids encoding HA-TBI and HA-TBII were a gift from J.L. Wrana (University of Toronto, Toronto, Canada).

Cloning of *Chmp5*

CHMP5 was copurified with IκBα from rabbit lung tissue extract. After separation on SDS-PAGE and silver staining, a 32-kD band was excised from the gel and trypsinized, and five peptides were microsequenced. One mouse EST (available from GenBank/EMBL/DDBJ under accession no. W51061) matched these peptides and was used as a probe to screen a mouse liver cDNA library. One clone containing the *Chmp5* open reading frame was obtained and an additional 5′ sequence was cloned by 5′ rapid amplification of cDNA ends.

Generation of *Chmp5*$^{+/-}$ mice and *Chmp5*$^{-/-}$ ES cells

Four *Chmp5* genomic clones were isolated from a 129/SvJ mouse genomic DNA library (Stratagene). The targeting vector consists of a 5.3-kb 5′ homology region and a 4.7-kb 3′ homology region. A loxP-PGKneo-loxP cassette was inserted between the two regions and a PGK-TK cassette was placed upstream of the 5′ homology region, resulting in a vector designed to delete exons 3–7 of *Chmp5*. Linearized targeting vector was electroporated into TC1 ES cells. Clones resistant to G418 and gancyclovir were selected, and homologous recombination was confirmed by Southern blotting. Two targeted clones were injected into C57BL/6 blastocysts and both produced germline chimeras. Chimeras were mated with C57BL/6 females, and heterozygous male offspring were bred with female *splicer* mice to delete the floxed neo cassette. Their offspring were screened for the targeted allele without the neo cassette and in the absence of the *cre* transgene. Positive mice were interbred and maintained on a mixed 129 × C57BL/6 background.

To establish *Chmp5*$^{-/-}$ ES cell lines, *Chmp5*$^{+/-}$ mice were mated, blastocysts were collected, and ES cell lines were isolated from the inner cell mass and cultured as previously described (Robertson, 1987). The genotypes of ES cell lines were determined by Southern blotting and immunoblotting with anti-CHMP5 antibody.

Whole-mount in situ hybridization and TUNEL assay

Whole-mount TUNEL assay and in situ hybridization using digoxigenin UTP-labeled riboprobes were performed as previously described (Sasaki and Hogan, 1993). Embryos were placed on 60-mm Petri dish containing 1% agarose that was filled with PBS and oriented as indicated. The embryos were imaged on a dissecting microscope (model Stemi 2000-C; Carl Zeiss MicroImaging, Inc.) using 16×/16, NA 2.5, objectives (AxioCam; Carl Zeiss MicroImaging, Inc.). Image data was acquired and stored as TIFF files using AxioCam software.

Isolation of cells from mouse embryos

E8.5 embryos from breeding of *Chmp5*$^{+/-}$ mice were dissected free of maternal tissues and had their Reichert's membrane removed, after which they were washed with PBS and incubated with 0.1% collagenase (Sigma-Aldrich) and Trypsin-EDTA (Invitrogen) for 30 min at 37°C. The cell suspension was plated in 24-well plates precoated with 0.2% gelatin (Sigma-Aldrich) and cultured in DME supplemented with 15% FBS (Sigma-Aldrich). *Chmp5*$^{-/-}$ cells were identified by immunostaining with CHMP5 antibody or PCR from extraembryonic tissues.

Transmission electron microscopy

E8.0–8.25 embryos were dissected and washed with PBS, and then fixed with 4% paraformaldehyde and 2% glutaraldehyde in 0.1 M sodium cacodylate buffer, pH 7.2, for 1 h at room temperature. Further procedures were performed by standard protocols.

Immunofluorescence

For immunofluorescence analysis, cells were grown on 0.2% gelatin-coated coverslips, washed with PBS, fixed with 4% paraformaldehyde for 30 min at room temperature, and permeabilized with permeabilization buffer (0.05% saponin, 1% FBS, 10 mM Hepes, and 10 mM glycine in PBS, pH 7.5) for 30 min at room temperature. Cells were incubated with the indicated primary antibodies for 30 min at room temperature and then incubated with either goat anti–rabbit or anti–mouse antibodies conjugated with FITC or Texas red under identical conditions. Subsequently, cells were washed three times with PBS, mounted in GEL/MOUNT (Biomeda), and examined under either a Plan Apochromat 63× oil objective or a Plan Neofluar 40× oil objective on a fluorescence microscope (Axioplan 2; all Carl Zeiss MicroImaging, Inc.) equipped with a charge-coupled device camera (Orca ER; Hamamatsu). Image data was acquired and stored as TIFF files using OpenLab software (Improvision, Inc.).

Generation of CHMP5 ShRNAs

shRNAs with murine CHMP5 target sequence Sh2 (5′-CCTGGCCCAACAGTCCTTT-3′) and murine CHMP5 control sequence Sh1 (5′-AAGCGAAACCCAAGGCTCC-3′), or human CHMP5 target sequence Sh3 (5′-AAGGACACCAAGACCACGGTT-3′) were produced by chemically synthesized DNA oligonucleotides and cloned into pSUPER.retro vector following the manufacturer's instruction (OligoEngine). To test ShRNAs, Flag-tagged *Chmp5* cDNA and CHMP5 ShRNAs were cotransfected into COS1 cells. 48 h after transfection, cells were lysed and immunoblotted with antibodies specific for Flag and GAPDH4.

Endosome–lysosome transport assay

NIH3T3 cells were cultured in medium containing protease inhibitors to inhibit protein degradation in lysosomes throughout the experiment. Cells were incubated with biotin-conjugated HRP for 3 h to label lysosomes before being transfected with CHMP5 shRNA. 48 h after transfection, cells were incubated with streptavidin for 10 min, washed, chased for the indicated time points, and lysed with biotin-containing lysis buffer. Lysates were applied to antistreptavidin-coated plates, incubated for 1 h, and washed; HRP enzymatic activity was measured by colorimetric assay and is expressed as arbitrary units.

Subcellular fractionation and protease protection assay

HEK293 cells were transfected with COOH-terminal HA-TβRII in the presence or absence of human CHMP5 shRNA (Sh3). 48 h after transfection, cells were treated with 10 ng/ml TGFβ for 5 h or left untreated and fractionated using Percoll gradients as previously described (Marsh et al., 1987). In brief, cells were washed and resuspended in homogenization buffer (10 mM triethanolamine, 10 mM acetic acid, 1 mM EDTA, and 0.25 M sucrose, pH 7.4) and disrupted with 20 strokes in a dounce homogenizer. Microscopic analysis assured that the cell breakage was nearly complete. The homogenate was centrifuged at 1,000 *g* for 5 min at 4°C to remove nuclei and unbroken cells. The postnuclear supernatant was mixed with Percoll (Sigma-Aldrich) in homogenization buffer to give a final concentration of 27%, and the mixture was underlaid with a 27.6% nycodenz solution (Sigma-Aldrich). The gradients were centrifuged in a SW41Ti rotor at 17,500 rpm for 1 h at 4°C, and 14 fractions were collected from the top of gradient.

Protease protection assays have traditionally been used to determine the sidedness of proteins relative to a sealed membrane compartments (Blobel and Sabatini, 1970; Sabatini and Blobel, 1970). These experiments typically involve the complete digestion of exposed domains of proteins on the outside of a sealed compartment and the protection of those domains or proteins that reside on the inside of the compartment (Wu et al., 2003; Sik et al., 2004). To apply the protease protection assay to our system, we modified the original protocol of the protease protection assay. For protease protection assay, 25-μl aliquots of each fraction were treated with 2–5 μg proteinase K for 30 min at room temperature or left untreated. The reaction was stopped by adding SDS loading buffer, and proteinase K was inactivated by boiling at 90°C. The samples were subjected to 10% SDS-PAGE, followed by immunoblotting with the indicated antibodies.

We would like to thank Crystal Bussey for technical assistance; Pietro De Camilli, Scott D. Emr, Walther Mothes, and Matthew B. Greenblatt for discussions; and Toshihide Kobayashi and Jeffrey L. Wrana for sharing reagents.

The work was supported by grants from the National Institutes of Health (R37-AI33443 and R37 AI-34098), the Ludwig Institute for Cancer Research (I. Mellman), and the American Heart Association (E.S. Trombetta). M.S. Hayden was supported in part by the National Institute of General Medical Sciences Medical Scientist Training Program training grant GM-07205.

Submitted: 7 September 2005
Accepted: 17 February 2006

References

Amerik, A.Y., J. Nowak, S. Swaminathan, and M. Hochstrasser. 2000. The Doa4 deubiquitinating enzyme is functionally linked to the vacuolar protein-sorting and endocytic pathways. *Mol. Biol. Cell*. 11:3365–3380.

Babst, M. 2005. A protein's final ESCRT. *Traffic*. 6:2–9.

Babst, M., B. Wendland, E.J. Estepa, and S.D. Emr. 1998. The Vps4p AAA ATPase regulates membrane association of a Vps protein complex required for normal endosome function. *EMBO J.* 17:2982–2993.

Babst, M., G. Odorizzi, E.J. Estepa, and S.D. Emr. 2000. Mammalian tumor susceptibility gene 101 (TSG101) and the yeast homologue, Vps23p, both function in late endosomal trafficking. *Traffic*. 1:248–258.

Babst, M., D.J. Katzmann, E.J. Estepa-Sabal, T. Meerloo, and S.D. Emr. 2002a. Escrt-III: an endosome-associated heterooligomeric protein complex required for mvb sorting. *Dev. Cell*. 3:271–282.

Babst, M., D.J. Katzmann, W.B. Snyder, B. Wendland, and S.D. Emr. 2002b. Endosome-associated complex, ESCRT-II, recruits transport machinery for protein sorting at the multivesicular body. *Dev. Cell*. 3:283–289.

Bilodeau, P.S., J.L. Urbanowski, S.C. Winistorfer, and R.C. Piper. 2002. The Vps27p-Hse1p complex binds ubiquitin and mediates endosomal protein sorting. *Nat. Cell Biol.* 4:534–539.

Bishop, N., and P. Woodman. 2001. TSG101/mammalian VPS23 and mammalian VPS28 interact directly and are recruited to VPS4-induced endosomes. *J. Biol. Chem.* 276:11735–11742.

Blobel, G., and D.D. Sabatini. 1970. Controlled proteolysis of nascent polypeptides in rat liver cell fractions. I. Location of the polypeptides within ribosomes. *J. Cell Biol.* 45:130–145.

Bowers, K., J. Lottridge, S.B. Helliwell, L.M. Goldthwaite, J.P. Luzio, and T.H. Stevens. 2004. Protein-protein interactions of ESCRT complexes in the yeast *Saccharomyces cerevisiae. Traffic*. 5:194–210.

Corson, L.B., Y. Yamanaka, K.M. Lai, and J. Rossant. 2003. Spatial and temporal patterns of ERK signaling during mouse embryogenesis. *Development*. 130:4527–4537.

Di Guglielmo, G.M., C. Le Roy, A.F. Goodfellow, and J.L. Wrana. 2003. Distinct endocytic pathways regulate TGF-beta receptor signalling and turnover. *Nat. Cell Biol.* 5:410–421.

Futter, C.E., L.M. Collinson, J.M. Backer, and C.R. Hopkins. 2001. Human VPS34 is required for internal vesicle formation within multivesicular endosomes. *J. Cell Biol.* 155:1251–1264.

Hayden, M.S., and S. Ghosh. 2004. Signaling to NF-κB. *Genes Dev.* 18:2195–2224.

Hayes, S., A. Chawla, and S. Corvera. 2002. TGFβ receptor internalization into EEA1-enriched early endosomes: role in signaling to Smad2. *J. Cell Biol.* 158:1239–1249.

Ilangumaran, S., D. Finan, J. La Rose, J. Raine, A. Silverstein, P. De Sepulveda, and R. Rottapel. 2002. A positive regulatory role for suppressor of cytokine signaling 1 in IFN-γ-induced MHC II expression in fibroblasts. *J. Immunol.* 169:5010–5020.

Katzmann, D.J., M. Babst, and S.D. Emr. 2001. Ubiquitin-dependent sorting into the multivesicular body pathway requires the function of a conserved endosomal protein sorting complex, ESCRT-1. *Cell*. 106:145–155.

Katzmann, D.J., G. Odorizzi, and S.D. Emr. 2002. Receptor downregulation and multivesicular-body sorting. *Nat. Rev. Mol. Cell Biol.* 3:893–905.

Kavsak, P., R.K. Rasmussen, C.G. Causing, S. Bonni, H. Zhu, G.H. Thomsen, and J.L. Wrana. 2000. Smad7 binds to Smurf2 to form an E3 ubiquitin ligase that targets the TGFbeta receptor for degradation. *Mol. Cell*. 6:1365–1375.

Kobayashi, T., E. Stang, K.S. Fang, P. De Moerloose, R.G. Parton, and J. Gruenberg. 1998. A lipid associated with the antiphospholipid syndrome regulates endosome structure and function. *Nature*. 392:193–197.

Kohler, J.R. 2003. Mos10 (Vps60) is required for normal filament maturation in *Saccharomyces cerevisiae*. *Mol. Microbiol.* 49:1267–1285.

Komada, M., and P. Soriano. 1999. Hrs, a FYVE finger protein localized to early endosomes, is implicated in vesicular traffic and required for ventral folding morphogenesis. *Genes Dev.* 13:1475–1485.

Koni, P.A., S.K. Joshi, U.A. Temann, D. Olson, L. Burkly, and R.A. Flavell. 2001. Conditional vascular cell adhesion molecule 1 deletion in mice: impaired lymphocyte migration to bone marrow. *J. Exp. Med.* 193:741–754.

Kornfeld, S., and I. Mellman. 1989. The biogenesis of lysosomes. *Annu. Rev. Cell Biol.* 5:483–525.

Kranz, A., A. Kinner, and R. Kolling. 2001. A family of small coiled-coil-forming proteins functioning at the late endosome in yeast. *Mol. Biol. Cell*. 12:711–723.

Lloyd, T.E., R. Atkinson, M.N. Wu, Y. Zhou, G. Pennetta, and H.J. Bellen. 2002. Hrs regulates endosome membrane invagination and tyrosine kinase receptor signaling in *Drosophila*. *Cell*. 108:261–269.

Lu, Q., L.W. Hope, M. Brasch, C. Reinhard, and S.N. Cohen. 2003. TSG101 interaction with HRS mediates endosomal trafficking and receptor down-regulation. *Proc. Natl. Acad. Sci. USA*. 100:7626–7631.

Luzio, J.P., B.A. Rous, N.A. Bright, P.R. Pryor, B.M. Mullock, and R.C. Piper. 2000. Lysosome-endosome fusion and lysosome biogenesis. *J. Cell Sci.* 113:1515–1524.

Martin-Serrano, J., A. Yaravoy, D. Perez-Caballero, and P.D. Bieniasz. 2003. Divergent retroviral late-budding domains recruit vacuolar protein sorting factors by using alternative adaptor proteins. *Proc. Natl. Acad. Sci. USA*. 100:12414–12419.

Marsh, M., S. Schmid, H. Kern, E. Harms, I. Mellman, and A. Helenius. 1987. Rapid analytical and preparative isolation of functional endosomes by free flow electrophoresis. *J. Cell Biol.* 104:875–886.

Mellman, I. 1996. Endocytosis and molecular sorting. *Annu. Rev. Cell Dev. Biol.* 12:575–625.

Mellman, I., and R.M. Steinman. 2001. Dendritic cells: specialized and regulated antigen processing machines. *Cell*. 106:255–258.

Paddison, P.J., A.A. Caudy, E. Bernstein, G.J. Hannon, and D.S. Conklin. 2002. Short hairpin RNAs (shRNAs) induce sequence-specific silencing in mammalian cells. *Genes Dev.* 16:948–958.

Polo, S., S. Sigismund, M. Faretta, M. Guidi, M.R. Capua, G. Bossi, H. Chen, P. De Camilli, and P.P. Di Flore. 2002. A single motif responsible for ubiquitin recognition and monoubiquitination in endocytic proteins. *Nature*. 416:451–455.

Raiborg, C., T.E. Rusten, and H. Stenmark. 2003. Protein sorting into multivesicular endosomes. *Curr. Opin. Cell Biol.* 15:446–455.

Raymond, C.K., I. Howald-Stevenson, C.A. Vater, and T.H. Stevens. 1992. Morphological classification of the yeast vacuolar protein sorting mutants: evidence for a prevacuolar compartment in class E vps mutants. *Mol. Biol. Cell.* 3:1389–1402.

Robertson, E.J. 1987. Teratocarcinomas and Embryonic Stem Cells: A Practical Approach. IRL Press, Oxford, UK. 268 pp.

Rossant, J., B. Ciruna, and J. Partanen. 1997. FGF signaling in mouse gastrulation and anteroposterior patterning. *Cold Spring Harb. Symp. Quant. Biol.* 62:127–133.

Ruland, J., C. Sirard, A. Elia, D. Macpherson, A. Wakeham, L. Li, J. Pompa, S.N. Cohen, and T.W. Mak. 2001. P53 accumulation, defective cell proliferation, and early embryonic lethality in mice lacking tsg101. *Proc. Natl. Acad. Sci. USA*. 98:1859–1864.

Sabatini, D.D., and G. Blobel. 1970. Controlled proteolysis of nascent polypeptides in rat liver cell fractions. II. Location of the polypeptides in rough microsomes. *J. Cell Biol.* 45:146–157.

Sasaki, H., and B.L. Hogan. 1993. Differential expression of multiple fork head related genes during gastrulation and axial pattern formation in the mouse embryo. *Development*. 118:47–59.

Seto, E.S., H.J. Bellen, and T.E. Lloyd. 2002. When cell biology meets development: endocytic regulation of signaling pathways. *Genes Dev.* 16:1314–1336.

Shiflett, S.L., D.M. Ward, D. Huynh, M.B. Vaughn, J.C. Simmons, and J. Kaplan. 2004. Characterization of Vta1p, a class E vps protein in *Saccharomyces cerevisiae. J. Biol. Chem.* 279:10982–10990.

Sik, A., B.J. Passer, E.V. Koonin, and L. Pellegrini. 2004. Self-regulated cleavage of the mitochondrial intramembrane-cleaving protease PARL yields Pβ, a nuclear-targeted peptide. *J. Biol. Chem.* 279:15323–15329.

Takayama, S., and J.C. Reed. 2001. Molecular chaperone targeting and regulation by BAG family proteins. *Nat. Cell Biol.* 3:E237–E241.

von Schwedler, U.K., M. Stuchell, B. Muller, D.M. Ward, H.-Y. Chung, E. Morita, H.-E. Wang, T. Davis, G.-P. He, D.M. Cimbora, et al. 2003. The protein network of HIV budding. *Cell*. 114:701–713.

Ward, D.M., M.B. Vaughn, S.L. Shiflett, P.L. White, A.L. Pollock, J. Hill, R. Schnegelberger, W.I. Sundquist, and J. Kaplan. 2005. The role of LIP5 and CHMP5 in multivesicular body formation and HIV-1 budding in mammalian cells. *J. Biol. Chem.* 280:10548–10555.

Wu, C.C., M.J. MacCoss, K.E. Howell, and J.R. Yates III. 2003. A method for the comprehensive proteomic analysis of membrane proteins. *Nat. Biotechnol.* 21:532–538.

Yoshimori, T., F. Yamagata, A. Yamamoto, N. Mizushima, Y. Kabeya, A. Nara, I. Miwako, M. Ohashi, M. Ohsumi, and Y. Ohsumi. 2000. The mouse SKD1, a homologue of yeast Vps4p, is required for normal endosomal trafficking and morphology in mammalian cells. *Mol. Biol. Cell*. 11:747–763.